Model and Analysis of Current Sensor Based on Tunnel Magnetoresistance (TMR) Suitable for SiC and GaN

Xu XP, Liu TZ, Zhu MN, Zhou YO, Lei XY, Bai JM, Wang JG, and P.P. Freitas

***Abstract*—The current sensor protects the electrical equipment by detecting the operating current of the device in real time and combining with the external circuit. There are many kinds of current sensors usually used Hall device in the last decades which had played an important role in a variety of applications. With the successful application of new magnetic devices AMR(Anisotropic Magneto Resistive), GMR(Giant Magneto Resistive), TMR(Tunnel Magnetoresistance) in the field of hard drives and the need for current sensor development, AMR, GMR, TMR gradually replace Hall devices and begin to be used in the design and production of current sensors.TMR has inherent advantages over Hall, AMR, GMR in terms of the size, sensitivity, temperature characteristics as well as quick response and has a broad application fields. The third generation of semiconductor materials SiC & GaN's characteristics need the matched current sensor with a faster level of response speed and lower pass-band phase difference. The characteristics of the current sensor based on TMR are just enough to meet the requirements of SiC & GaN devices. So it is of great significance to model and analysis of TMR current sensors.**

***Index Terms*—current sensor, SiC & GaN, response speed, phase difference, model, analysis, AMR, GMR, TMR.**

I. Introduction

MANY types of devices are used to measure current and magnetic fields such as Hall, GMR, AMR, TMR[3]-[5]. TMR is a new kind of the magnetoresistance effect device,which is made by the magnetic multi-layer film material based on the tunnel magnetoresistance effect and has been widely used in industries. Hall is with inherent defects of lower sensitivity, higher power consumption and poor linearity. Although the sensitivity of AMR is much higher than that of Hall, its linearity range is narrow, and the AMR-based magnetic sensor needs to be set / reset by the set / reset coil, resulting in complicated manufacturing process. Although GMR has higher sensitivity than Hall, but its linear range is low. TMR is with advantage of better temperature stability, higher sensitivity, lower power consumption and better linearity than Hall, AMR, and GMR. TMR has been successfully used in the industry of the hard disk[6]-[7], proving that TMR is tech-matured and tech-advanced.

Xu XP and Liu TZ are with the school of Mechatronic Engineering and Automation, Shanghai University, Shanghai 200072, China(e-mail: liutzh@staff.shu.edu.cn).

Zhu MN, Zhou YO and Lei XY are with LerTech Technology Co., Ltd, Wuxi 214071, China.

Bai JM and Wang JG are with Sinomags Technology Co., Ltd, Ningbo 315200, China.

P. P. Freitas is with Institute de Engenharia de Sistemas e Computadores, Rua Alves Redol, 9, 1º Dt., P-1000 Lisboa, Portugal.

Device Performance Characteristics						
Device	Power consumption (mA)	Scope (Gs)	Sensitivity (mV/V/Gs)	Resolution (mGs)	Response time	Temperature (℃)
Hall	5~20	1~1000	0.05	100	2uS	<150℃
AMR	1~10	0.001~10	3	0.1	10nS	<150℃
GMR	1~10	0.1~30	3	0.1	10nS	<150℃
TMR	0.001~0.01	0.001~200	15	0.1	2nS	<200℃

TABLE. 1 Device performance characteristics

TMR has a significant comprehensive performance in TABLE.1.

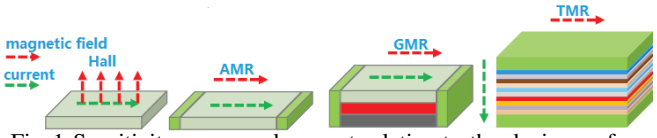

Fig. 1 Sensitivity, measured current relative to the device surface direction

In Fig.1 we can see that the direction of sensitivity of Hall is perpendicular to its surface, and the direction of sensitivity of AMR, GMR, TMR is parallel to their surfaces. So there are many advantages for the use of AMR, GMR, TMR in current sensor than Hall, especially in the application of non-core current sensor[8] has obvious inherent advantages. The third generation of power devices represented by SiC & GaN has faster response speed, higher power density and wider band-gap voltage, and are being widely used. Through practical research, SiC & GaN users require matching current sensor with a response time which is no more than 200ns and a phase difference which is no more than 40 degrees through the 500kHz bandwidth. TMR has a response time of up to 2ns[1] to meet the operating frequency requirements of SiC & GaN. In order to better evaluate the performance of TMR-based current sensors, three kinds of TMR current sensors were designed and developed, including two kinds of coreless open-loop current sensors SKT-1LP2, SKT-2DP2 and closed-loop current sensor STB-BS with magnetic core.

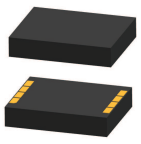

Fig. 2(a) SKT-1LP2

Fig. 2(b) SKT-2DP2

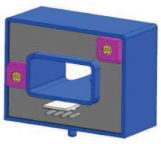

Fig. 2(c) STB-BS

II. SYSTEM DESIGN

A. TMR Structure and Package

TMR devices used in the experiments are produced by Sinomags Technology Co., LTD in China. TMR is divided into high sensitivity TMR and low sensitivity TMR. SKT-1LP2, SKT-2DP2 use low sensitivity TMR and STB-BS uses high sensitivity TMR. Due to the similar processing technology, the high sensitivity TMR and the low sensitivity TMR have similar frequency response, -3dB bandwidth, linearity and temperature characteristics in the respective saturation magnetic field range, except for the sensitivity difference. The sensitivity of the low sensitivity TMR is 0.1mV/V/A and the saturation magnetic field is 200 gauss. The sensitivity of the high sensitivity TMR is 3mV/V/A and the saturation magnetic field is 50 gauss. TJ1856 and DSI2119 are the low sensitivity TMR, SML320-C is the high sensitivity TMR. Each SKT-1LP2 uses two TJ1856s, each SKT-2DP2 uses two DSI2119s and each STB-BS uses one SML-320C. The TMR chip package includes COB whose size is 0.5*0.5*0.2mm and DFN whose size is 1*3*0.75mm. TMR TJ1856's package is COB; TMR DSI2119 and SML-320C's packages are DFN. Each DFN package includes two TMR dies. DSI2119 includes two TJ1856s.

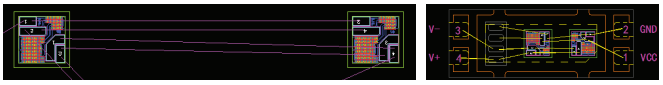

Fig. 3(a) Two-TJ1856 connection; Fig. 3(b) DFN connection

Two-TJ1856 and DFN's connections are showed in Fig.3. In Fig.4 Two-TJ1856 and Two-DSI2119 which is used one arm on each side of DNF4 are both designed as gradient magnetic field chips for the open-loop current sensor and the magnetic field at the two arms of Two-TJ1856 and DSI2119 is opposite. SML-302C is designed as absolute magnetic field chips for the closed-loop current sensor and the magnetic field at the two arms of SML-320C is the same in Fig.4.

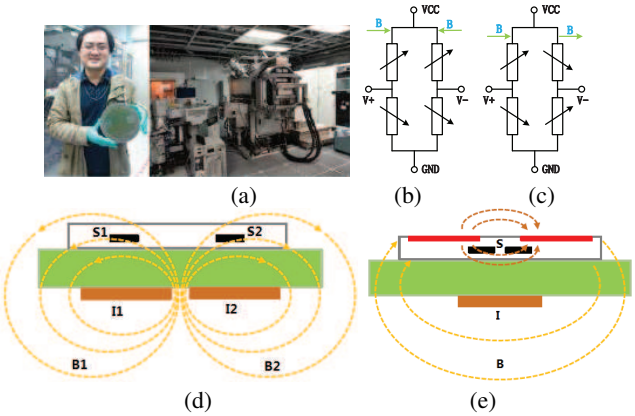

Fig. 4(a) Wafer and equipment; Fig. 4(b) gradient magnetic field structure of Two-TJ1856 or Two-DSI2119; Fig. 4(c) absolute magnetic field structure of SML-320C; Fig. 4(d) gradient magnetic field diagram; Fig. 4(e) absolute magnetic field diagram

TJ1856 and DSI2119 are made by the same low sensitivity TMR wafers and their performance are basically the same. SML-320C is made by the high sensitivity TMR wafers. Two-TJ1856 and Two-DSI2119 work in a gradient magnetic field, SML-302C works in a absolute magnetic field. Two-TJ1856, Two-DSI2119 and SML-302C are sensitive magnetic chips, using a unique push-pull wheatstone bridge design, and have a good temperature characteristics and anti-common-mode signal interference.

B. Magnetic field distribution characteristics of open-loop current sensor

SKT-1LP2 and SKT-2DP2 are TMR open-loop current sensors. SKT-1LP2's package is LGA which isn't integrated with current conductor inside while SKT-2DP2'package is DIP which is integrated with current conductor inside. Fig.5 is the 3D models of SKT-1LP2 and SKT-2DP2.

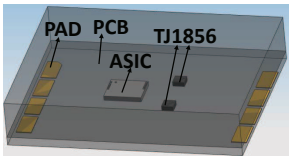

Fig. 5(a) SKT-1LP2

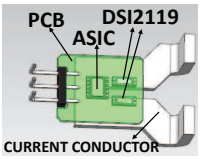

Fig. 5(b) SKT-2DP2

SKT-1LP2 and SKT-2DP2 work in the same principle. As the shape and position of SKT-2DP2 current conductor fixed, we mainly analyze the magnetic field characteristics of SKT-2DP2. The magnetic field characteristics of SKT-1LP2 are determined by the shape and position of the external current conductor. For details, refer to SKT-2DP2. With the center of the two TMR as the origin, the x axis and the y axis are shown in Fig.6.

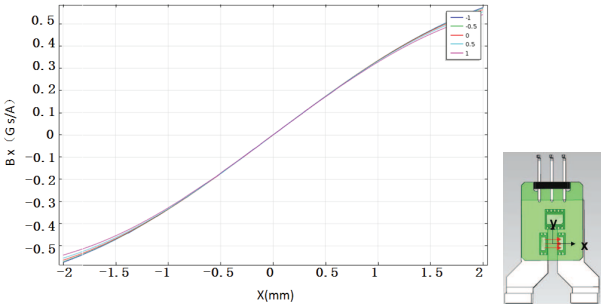

Fig. 6(a) SKT-2DP2 magnetic field sensitivity distribution in the x axis

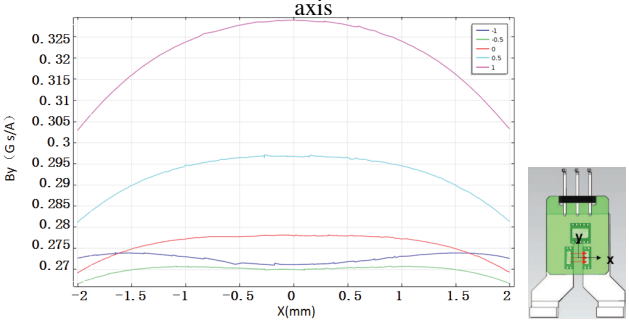

Fig. 6(b) SKT-2DP2 magnetic field sensitivity distribution in the y axis

In Fig.6 the coordinates of the two TMRs are (-1.3,0), (1.3,0), the nearest distance of the small edge of the current conductor edge is 2.6 from the origin, and the coordinate unit is mm. Bx and By represents the sensitivity of the current sensor in the x direction and the y direction respectively and their units are Gaussian per ampere. The simulation results in

Fig.6 show that the influence by By gradually decreases with the distance in the y direction within a certain range.

C. Magnetic field distribution characteristics of closed-loop current sensor

STB-BS is the closed-loop current sensor with a high sensitivity TMR SML-320C.

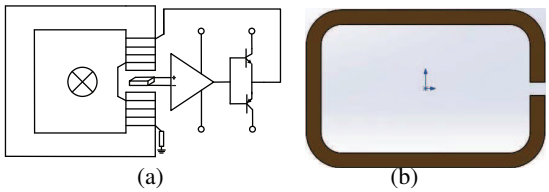

(a) (b)

Fig. 7(a) STB-BS's structure; Fig. 7(b) STB-BS's permalloy magnetic core

Fig.7(a) shows the structure of the TMR closed-loop current sensor STB-BS. This structure is similar to Hall or GMR closed-loop current sensor[2]. But the corresponding compensation circuit parameters are different due to TMR's unique characteristic. Circuit parameters are based on theoretical calculations and practical engineering experiences. Fig.7(b) shows the permalloy magnetic core, and the size of the core cross-sectional area is 2 * 2 mm. The core material is permalloy 1J85.

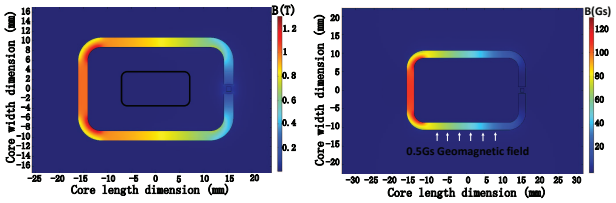

(a) (b)

Fig. 8 Magnetic field distribution of the single magnetic core regardless of the feedback coil and the core saturation

Fig.8(a) shows the magnetic field distribution of the core when 100A DC current is being passed through the center of the core, regardless of the feedback coil and the core saturation. In Fig.8(a) we can figure out the circuit magnification. Fig.8(b) shows the effect of the 0.5 Gaussian magnetic field in the core regardless of the feedback coil.

Actually due to the feedback coil, the entire closed-loop system is in magnetic balance and the magnetic field strength of the core air gap is near at zero in normal working conditions. So the core does not have a large magnetic field even at the center of the core passed by 100A DC current.

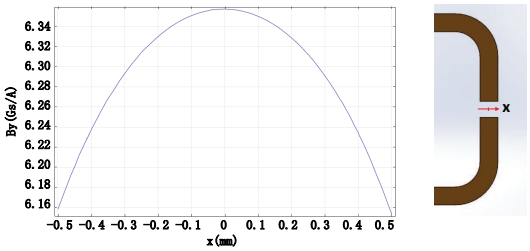

Fig. 9(a) Magnetic field strength in the x axis of the core air gap

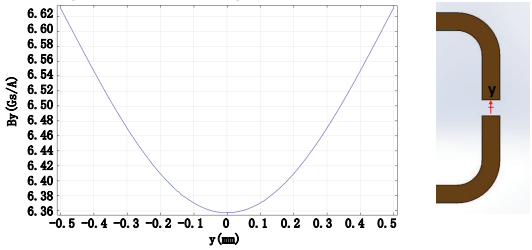

Fig. 9(b) Magnetic field strength in the y axis of the core air gap

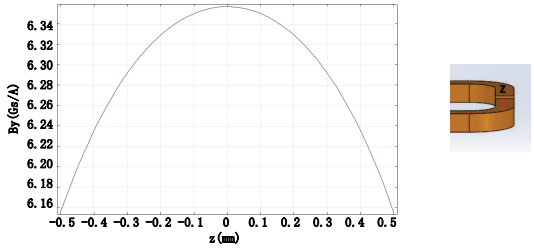

Fig. 9(c) Magnetic field strength in the z axis of the core air gap

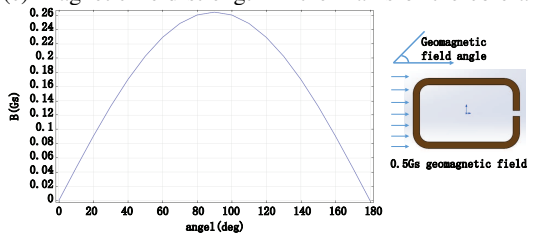

Fig. 9(d) Magnetic field strength of the core air gap affected by 0.5 Gaussian geomagnetic field with different angles.

The zero points in the x, y, and z directions are taken from the center of the core air gap. Bx, By, Bz represent the sensitivity of the core in x, y and z axis respectively, in units of Gaussian per ampere.

D. The model and transfer of open-loop current sensor based on TMR

The ASIC in Fig.5 integrated with LDO is a programmable op amp with programmable gain from 1.67 to 960 followed by an offset compensation DAC. It's model is NSA6000 produced by Sinomags Technology Co., LTD. Fig.10 shows the connection of Two-TJ1856 and ASIC-NSA6000 for SKT-1LP2 or the connection of Two-DSI2119 and ASIC-NSA6000 for SKT-2DP2.

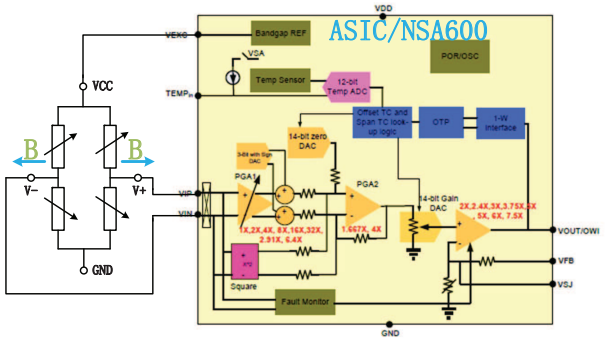

Fig. 10 Structure of SKT-1LP2 or SKT-2DP2

SKT-1LP2 or STK-2DP2 works in gradient magnetic field in Fig.10.

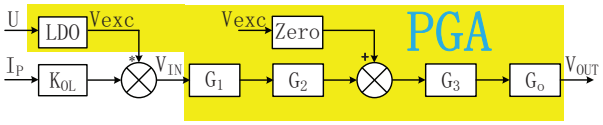

Fig. 11 The principle of SKT-1LP2 or SKT-2DP2

The transfer of open-loop current sensor based on TMR for SKT-1LP2 or SKT-2DP2 is equation (1). U is usually 5V in Fig.11.

$$V_{OUT} = (V_{IN} * G_1 * G_2 + V_{exc} * Z_{ero}) * G_3 * G_o \quad (1)$$

G_1 is the gain of the first stage of NSA6000 and can be chosen as 1, 2, 2.91, 4, 6, 6.4, 8, 16 and 32. G_2 is the gain of the second stage of NSA6000 and can be chosen as 1.667 and 4. V_{exc} is the LDO's output of NSA6000 which value is 4.096V. Z_{ero} is the scale factor of the ZERO DAC and can be calculated as ZDAC$/2^{14}$. G_3 is the scale factor of NSA6000 and its range is 1/3∼1. G_o is the gain of the last stage of NSA6000 and can be chosen as 2, 2.4, 3, 3.75, 5, 6 and 7.5. V_{IN} is Two-TJ1856 or Two-DSI2119's output and be expressed equation(2).

$$V_{IN} = V_{exc} * K_{OL} * I_P \quad (2)$$

K_{OL} is Two-TJ1856 or Two-DSI2119's sensitivity and its value is typically 0.1mV/V/A. I_P is the primary current. According to I_P, SKT-1LP2 or SKT-2DP2 can be configured by the different parameters.

E. The model and transfer of closed-loop current sensor based on TMR

In addition to the differences in the sensing device, the principle of the closed-loop current sensor is the same.

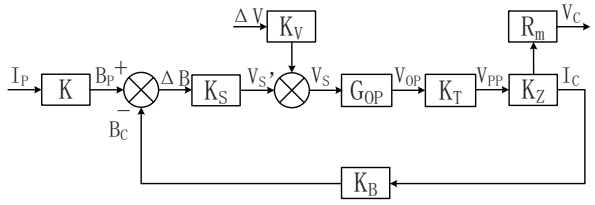

Fig. 12 The principle of STB-BS

Fig.12 shows the model of STB-BS and its transfer is equation(3) [2] when ΔV is zero .

$$\frac{I_C(s)}{I_P(s)} = \frac{N_1/N_2}{1 + \frac{t_{op}R_{tot}}{K_S K_B K_o p}s} \quad (3)$$

$$K_B = \frac{B_C}{I_C} = \frac{\mu_0 \mu_R N_2}{\pi D_C} \quad (4)$$

K_{OP} is the the static gain, t_{op} is the time constant of OP. R_{tot}=R_m+R_c, and R_c is the equivalent resistance of feedback winding and its typical value is about 20Ω. R_m is the sampling resistor. K_S is the sensitivity of SML-320C and its typical value is 3mV/V/A. K_B is expressed in equation(4). D_C is approximately the radius of the core in Fig.8.

When the supply voltage of TMR is not changed during the working time, ΔV is equal to zero. Then the output of TMR is equation(5). The output of OP is equation(6).

$$V_S = K_S * V_S' \quad (5)$$

$$V_{OP} = K_{OP} * K_S * V_S \quad (6)$$

When the supply voltage of TMR is changed during the working time, ΔV is not equal to zero. Then the output of TMR is equation (7). The output of OP is equation (8).

$$V_S = K_V * \Delta V + K_S * V_S' \quad (7)$$

$$V_{OP} = K_{OP} * (K_V * \Delta V + K_S * V_S') \quad (8)$$

K_{OP} is the static gain of OP whose value is typically 100dB and is intended to infinite, so equation (6) is equal to equation (8). So the output of STB-BS does not change within a reasonable range of the TMR supply voltage. In this condition the output of STB-BS is stable after actual measurement and is consistent with theoretical analysis.

III. Test Result

A. TMR Test Result

Fig.13 shows the accuracy of the low sensitivities TMR and the high sensitivities TMR at different magnetic field strength at 25°C.

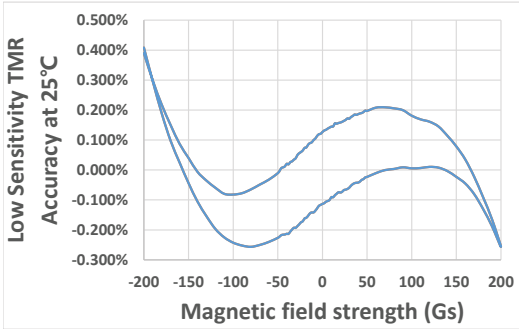

Fig. 13(a) Accuracy of low sensitivities TMR in 200Gs magnetic field

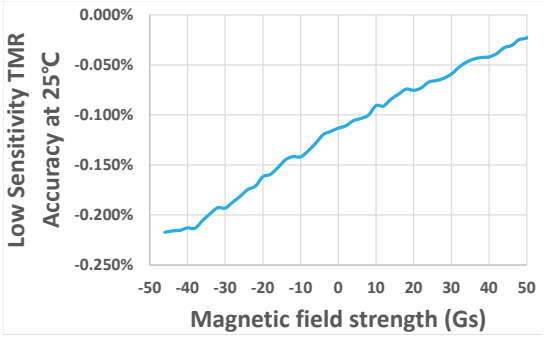

Fig. 13(b) Accuracy of low sensitivities TMR in 50Gs magnetic field

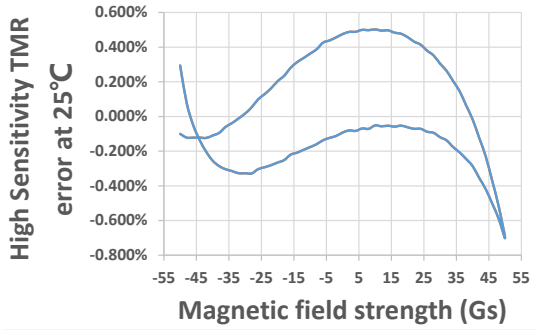

Fig. 13(c) Accuracy of high sensitivities TMR in 50Gs magnetic field

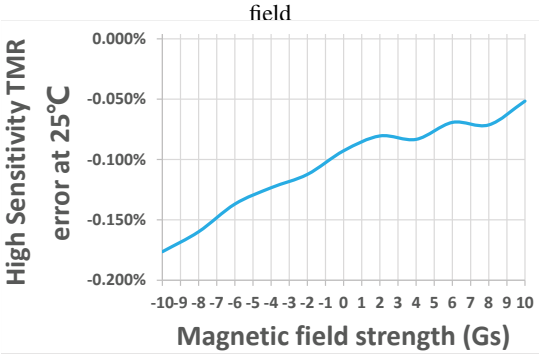

Fig. 13(d) Accuracy of high sensitivities TMR in 10Gs magnetic field

TMR works better in small magnetic fields relatively in Fig.13. Usually, the high sensitivity TMR for STB-BS works in less than 10 Gaussian magnetic field and low sensitivity TMR for SKT-1LP2 or SKT-2DP2 works in less than 100 Gaussian magnetic field. So their accuracy is good.

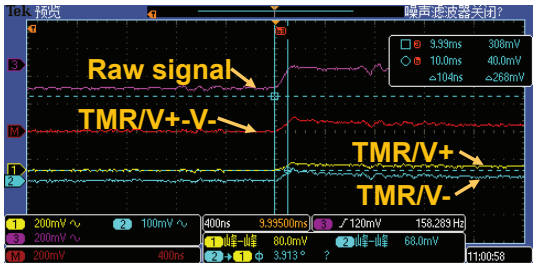

Fig. 14(a) The frequency response of TMR

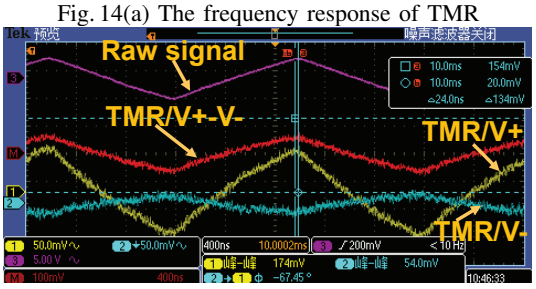

Fig. 14(b) The low triangular phase difference at 500kHz

In Fig.14, TMR SML-320C is tested in the absolute magnetic field. We can see that TMR response time is less than 100ns and the phase difference of the triangular wave at 500kHz is not greater than 5 degrees. These properties meet the performance requirements of SiC and GaN.

B. SKT-1LP2 and SKT-2DP2 DC Test Result

NSA6000 internal integrated temperature sensor, complies with the whole temperature zone in the respect of the TMR temperature compensation as well as correction and optimization of the open-loop current sensor full-temperature performance. SKT-1LP2 and SKT-2DP2 typical tests are used the same current conductor in Fig.5(b). Typical configuration parameters of SKT-1LP2 and SKT-2DP2 are in TABLE.2.

SKT-1LP2 Typical Configuration Parameters						
Temperature	G_1	G_2	G_0	Zero	G_3	Temperature Register
-40℃	4	1	1	0.397566	0.6687	02C0
-30℃	4	1	1	0.401947	0.6605	02DE
0℃	4	1	1	0.410562	0.6408	0339
25℃	4	1	1	0.413	0.6339	0388
50℃	4	1	1	0.408154	0.6396	03D4
70℃	4	1	1	0.398001	0.6549	0411
85℃	4	1	1	0.388291	0.6733	043F
105℃	4	1	1	0.373877	0.7108	047E
Remarks: Primary current 25A, output 2.5±0.5V.						

TABLE. 2(a) Typical configuration parameters of SKT-1LP2

SKT-2DP2 Typical Configuration Parameters						
Temperature	G_1	G_2	G_0	Zero	G_3	Temperature Register
-40℃	4	1	1	0.23771	0.639	02D8
-30℃	4	1	1	0.24198	0.632	02F5
0℃	4	1	1	0.25358	0.615	034E
25℃	4	1	1	0.25487	0.613	039F
50℃	4	1	1	0.24772	0.625	03E7
70℃	4	1	1	0.23541	0.646	0427
85℃	4	1	1	0.22259	0.668	0456
105℃	4	1	1	0.202	0.706	0493
Remarks: Primary current 25A, output 2.5±0.5V.						

TABLE. 2(b) Typical configuration parameters of SKT-2DP2

In TABLE 2, the PGA of SKT-1LP2 or SKT-1LP2 is magnified about 90 times. Due to the individual differences of each NSA6000, the initial value of the temperature register is different, but the absolute value of the temperature change in the whole temperature range is basically less than 5°C. SKT-1LP2 fast frequency response series prototype is being developed. SKT-2DP2 fast frequency response series prototype was tested below.

By configuring the relevant parameters, both SKT-1LP2 and SKT-2DP2 can be configured as fast response series and relatively slow response series by the theoretical analysis. The difference is mainly frequency response and bandwidth, but there is no significantly different in the respect of temperature characteristics and full temperature range accuracy. Slow frequency response series frequency is 1.5us, -3dB bandwidth is 500kHz; fast frequency response series frequency response is 100ns, -3dB bandwidth is not less than 1MHz. At the same time with the characteristics of small size.

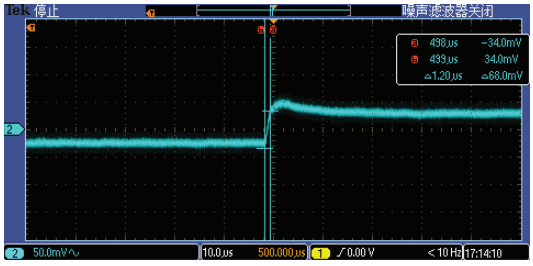

Fig. 15(a) Slow frequency response of SKT-1LP2

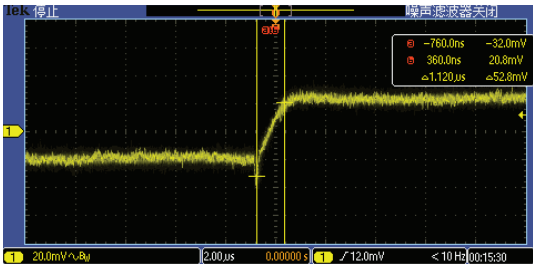

Fig. 15(b) Slow frequency response of SKT-2DP2

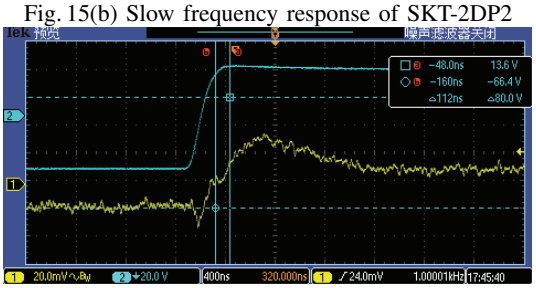

Fig. 15(c) Fast frequency response of SKT-2DP2

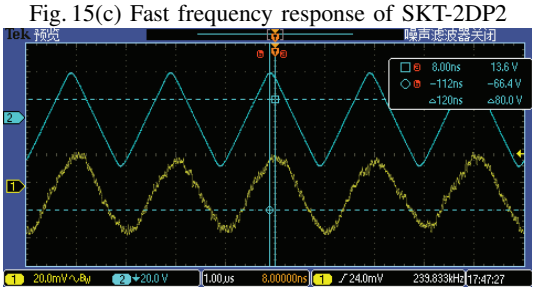

Fig. 15(d) Low delay for 500kHz triangular wave of SKT-2DP2

By adjusting the circuit parameters and the magnetic field characteristics near the wire, we can get the different frequency response in Fig.15. Fast frequency response is generally accompanied by overshoot in open-loop current sensors. Frequency response can reach 100ns or less, but the minimum amplitude of the overshoot is about 80% of the normal signal amplitude. Subsequent need be further optimized. In a certain range of overshoot, the open-loop current sensor's performance of linearity and accuracy does not change significantly. The following linearity and accuracy of the test data are based on slow frequency response of the open loop current sensor.

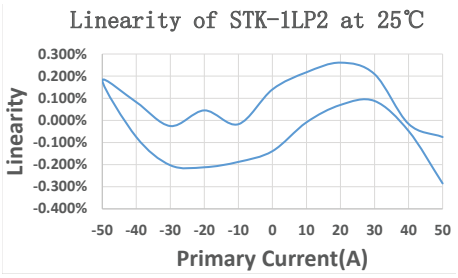

Fig. 16(a) Linearity of SKT-1LP2 at 25°C

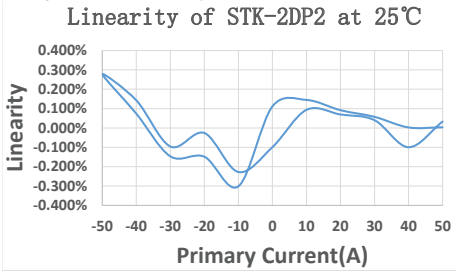

Fig. 16(b) Linearity of SKT-2DP2 at 25°C

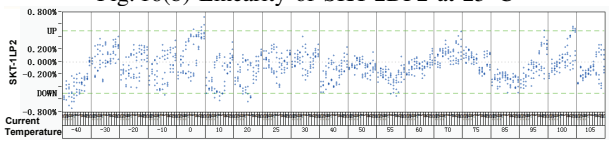

Fig. 16(c) Accuracy of SKT-1LP2 from 25°C to 105°C

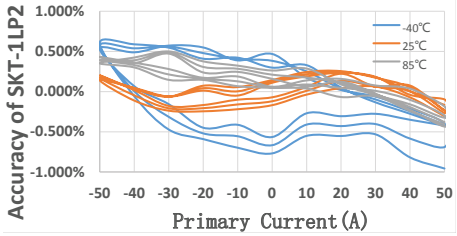

Fig. 16(d) Partial magnification for the accuracy of SKT-1LP2 from 25°C to 85°C

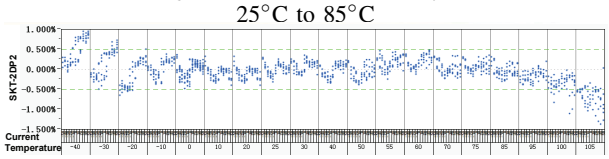

Fig. 16(e) Accuracy of SKT-2DP2 from 25°C to 105°C

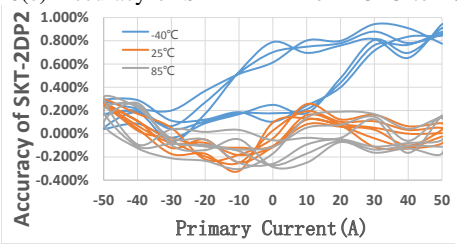

Fig. 16(f) Partial magnification for the accuracy of SKT-2DP2 from 25°C to 85°C

SKT-1LP2 and SKT-2DP2's linearity is less than 0.35% at 25°C in Fig.16. SKT-1LP2 and SKT-2DP2's accuracy is within 0.5% at 25°C. Their accuracy in full temperature range is within 1.5%, especially is with 1% below 85°C.

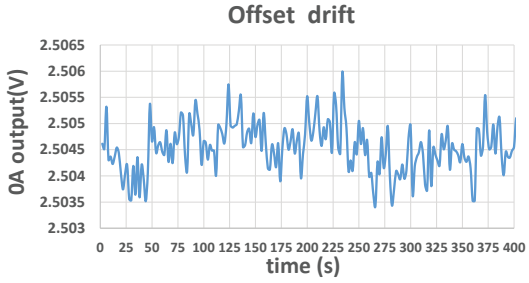

Fig. 17(a) Offset drift of SKT-1LP2

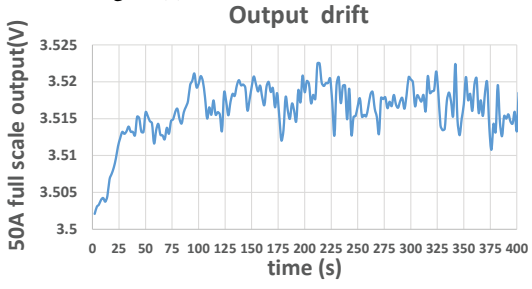

Fig. 17(b) Full scale drift of SKT-1LP2

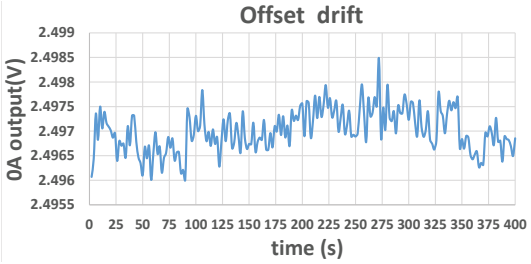

Fig. 17(C) Offset drift of SKT-2DP2

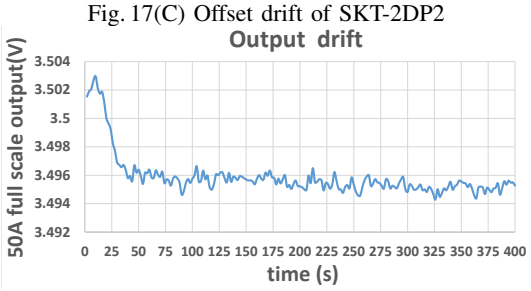

Fig. 17(d) Full scale drift of SKT-2DP2

Long time power test at 25°C, SKT-1LP2 and SKT-2DP2 offset noise is tested within 3mV. Long time power and passing the 50A DC current test at 25°C, SKT-1LP2 full-scale drift is tested within 25mV, SKT-2DP2 full-scale drift is less than 10mV. In this experiment, the temperature rise of the current conductor is 40°C. The temperature characteristics of SKT-1LP2 need be optimized.

C. STB-BS DC Test Result

The size of the magnetic core is shown in Fig.8. Feedback coil with 0.018mm diameter of the enameled wire wrapped in the core frame wrapped around the 2000 laps and its resistor is about 20Ω. When the primary current I_P is 200A, the feedback current I_C is 100mA.

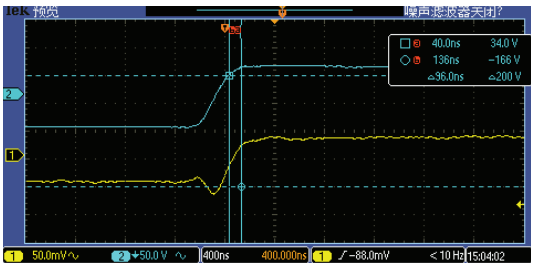

Fig. 18(a) STB-BS rise time

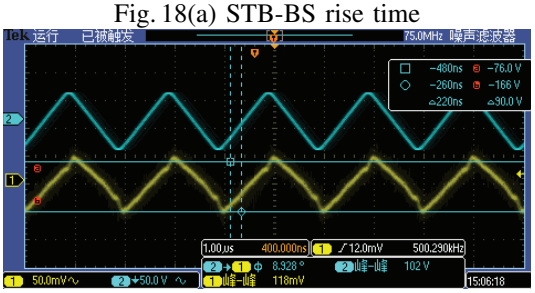

Fig. 18(b) Low delay for 500kHz triangular wave of STB-BS

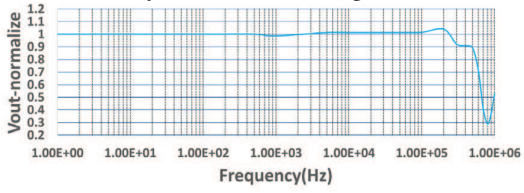

Fig. 18(c) STB-BS bandwidth

STB-BS's response time is about 100ns and the phase difference of the triangular wave at 500kHz is not greater than 40 degrees. Its bandwidth is 600kHz. These characters is very suitable for SiC & GaN device. In order to minimize the impact of remanence and other factors concurrently improve the accuracy of the test, the order of each measurement cycle is 200A ∼ 0A ∼ -200A ∼ 0A ∼ 200A and circulate three times.

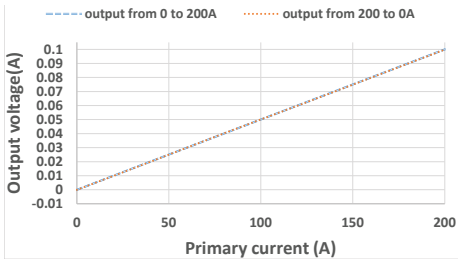

Fig. 19(a) Input and output characteristic curves of STB-BS

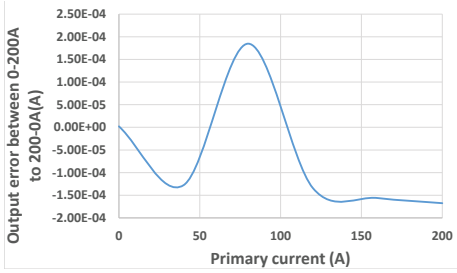

Fig. 19(b) Measured positive current and negative current absolute value difference of STB-BS

There is about max 20uA between the 0A∼ 200A loop and the 200A∼ 0A loop. The difference is caused by the core hysteresis.

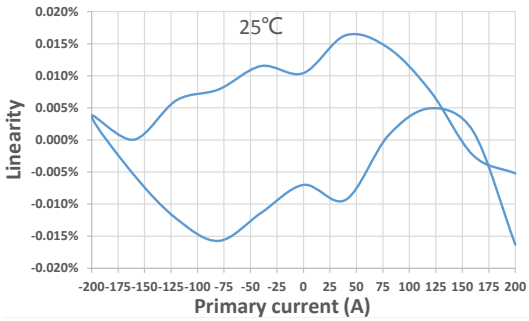

Fig. 20(a) Linearity of sensor at room temperature 25 °C

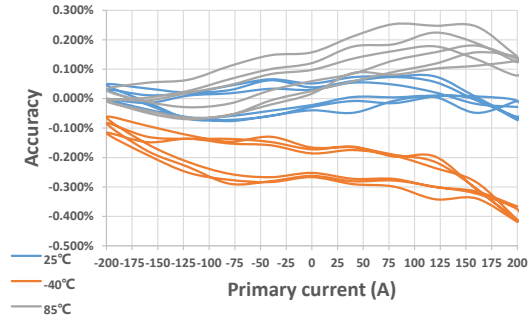

Fig. 20(b) Accuracy of sensor at temperature 25 °C,-40 °C and 85 °C

The linearity of the sensor is less than 0.03% at room temperature 25°C and the relative error of the sensor is less than 0.5% between -40 °C and 85 °C.

All the test data proves the excellent characteristics of the TMR current sensors. Fast frequency response of the open-loop current sensor STK-2DP2 and STB-BS closed-loop current sensor's performance is capable of meeting the working characteristics of the third generation of power devices SiC and GaN.

The open-loop current sensor SKT-1LP2 with fast frequency response series is being developed. TMR current sensors such as SKT-1LP2, SKT-2DP2 and STB-BS can also be used in AC field. The performance in AC field is usually better than DC at the same condition. The test results in AC field are shown in future.

ACKNOWLEDGMENT

The authors would like to thank Chen HY, Chen SN, Zhu HH, Dr. Yang ZJ and Dr. Mao SN. The work went well under their guidance and help.

REFERENCES

[1] H.w. Schumacher, C Chappert, R.C. Sousa and P.P. Freitas, *"Effective bit addressing tiems for precessional switching of magnetic memory cells"*,J. Appl. Phys. 97, 123907, pp.1-7, JUNE, 2005.

[2] Xiaoguang Yang, Hang Liu, Yuanyuan Wang, Youhua Wang, Guoya Dong and Zhenghan Zhao, *"A Giant Magneto Resistive (GMR) Effect Based Current Sensor With a Toroidal Magnetic Core as Flux Concentrator and Closed-Loop Configuration"*,IEEE Trans. Ind. Appl.,vol. 24,no. 3, pp. 901-909, JUNE, 2014.

[3] J. Lenz and A. S. Edelstein, *"Magnetic sensors and their applications,"*,IEEE Sensors J., vol. 6, no. 3, pp. 31-649, Jun. 2006.

[4] C. Xiao, L. Zhao, T. Asada, W. G. Odendaal, and J. D van Wyk, *"An overview of integratable current sensor technologies,"*, in Conf. Rec. 38th IAS Annu. Meeting, Oct. 2003, vol. 2, pp. 1251-1258.

[5] R. S. Popovic, J. A. Flanagan, and P. A. Besse, *"The future of magnetic sensors,"*, Sens. Actuators A, Phys., vol. 56, no. 1/2, pp. 39-55, Aug. 1996.

[6] J. M. Daughton and Y. J. Chen, *"GMR materials for low field applications,"*, IEEE Trans. Magn., vol. 29, no. 6, pp. 2705-2710, Nov. 1993.

[7] A. Edelstein, *"Advances in magnetometry,"*, J. Phys., Condens. Matter., vol. 19, no. 16, pp. 165217-165244, Apr. 2007.

[8] E. R. Olson and R. D. Lorenz, *"Effective use of miniature multipoint field-based current sensors without magnetic cores,"*, IEEE Trans. Ind. Appl., vol. 46, no. 2, pp. 901-909, Mar./Apr. 2010.